Letter to the Editor

A monoallelic activating mutation in *RAC2* resulting in a combined immunodeficiency

To the Editor:

The Rho guanosine triphosphatases, RAC1, RAC2, and RAC3, regulate cellular functions by switching from the inactive guanosine diphosphate–bound state to the active guanosine triphosphate–bound state.[1] RAC1 and RAC3 are widely expressed, whereas RAC2 is expressed only in hematopoietic cells.[1] The mouse model of RAC2 deficiency and patients with the dominant negative $RAC2^{D57N}$ mutant have neutrophilia, recurrent abscesses, and defective wound healing.[2,3] Because of the contribution of RAC2 to the function of the glyceraldehyde-3-phosphate dehydrogenase oxidase complex, $RAC2^{D57N}$ impairs the generation of superoxide in neutrophils. $RAC2^{D57N}$ also disrupts the polymerization of filamentous actin, thereby reducing myeloid cell and lymphocyte chemotaxis and adhesion.[2,3] Although conditional deletion of either RAC1 or RAC2 in lymphocytes is sufficient for intact T-cell and B-cell development in mice, reduced numbers of $CD4^+$ T cells and B cells have been found in one patient with $RAC2^{D57N}$ and in another kindred lacking RAC2 protein expression due to a homozygous $RAC2^{W56X}$ mutation.[4,5] Somatic activating variants in *RAC2* have been associated with melanoma,[1] but there are no published reports of germline gain-of-function mutations in any RAC family members. Here, we report a monoallelic germline gain-of-function $RAC2^{P34H}$ mutant in a family with a combined immunodeficiency.

Patient 1 is a 39-year-old man with a history of bronchiectasis, recurrent sinopulmonary infections, cutaneous human papillomavirus infections, and basal cell carcinomas. At age 34 years, he developed antiphospholipid syndrome and an IgM monoclonal gammopathy in association with a low-grade B-cell non-Hodgkin lymphoma, which was treated with rituximab, cyclophosphamide, doxorubicin, vincristine, and prednisone. His daughters (patients 2 and 3; Fig 1, *A*) had a history of recurrent sinopulmonary infections, severe lymphopenia since early childhood, and mild intermittent neutropenia (see Fig E1, *A*, in this article's Online Repository at www.jacionline.org). All patients are undergoing treatment with immunoglobulin replacement and antibiotic prophylaxis. The patients had reduced $CD4^+$ and $CD8^+$ T cells, recent thymic emigrants, naive T cells, and proliferative responses to stimulation with mitogens (Table I). All 3 patients had an accumulation of senescent $CD8^+CD57^+$ T cells (Table I). The patients had low $CD19^+$ B cells. Immunoglobulin levels before initiation of immunoglobulin replacement were available for patients 2 and 3. They demonstrated hypogammaglobulinemia and undetectable titers to tetanus and hepatitis vaccines (Table I). Collectively, these findings indicate a combined immunodeficiency.

Whole-exome sequencing on all 3 patients identified 51 rare deleterious variants shared by all 3 patients (see Table E1 in this article's Online Repository at www.jacionline.org). Of these, a heterozygous missense mutation in *RAC2* (NM_002872: c.C101A; p.P34H) was considered a plausible candidate due to the importance of RAC2 in immune cell function. The mutation was confirmed by Sanger sequencing (Fig 1, *B*) and had a deleterious Combined Annotation Dependent Depletion Phred-like score of 32.[7] The mutated P34 residue resides within the highly conserved Switch 1 domain important for interactions with guanine exchange factors and downstream effectors (Fig 1, *C*).[1] Immunoblotting revealed similar levels of RAC2 in patients and controls (Fig E1, *B*). Because the patients' primary cells express both wild-type (WT) and $RAC2^{P34H}$, we expressed Flag-tagged WT or mutant RAC2 in HEK293T cells and confirmed that WT and mutant forms of RAC2 had comparable expression (Fig 1, *D*). Modeling of $RAC2^{P34H}$ suggested a potential interaction between guanosine triphosphate and P34H, which would stabilize the binding of active RAC2 to effector proteins (Fig 1, *E*). $RAC2^{P34H}$ had increased binding to the effector protein PAK compared with WT RAC2, which was reversed by loading with endogenous guanosine diphosphate (Fig 1, *F*). $RAC2^{P34H}$ therefore has a gain-of-function effect.

RAC2 regulates the activity of the actin depolymerizing protein cofilin.[1] Dominant negative or loss-of-function mutations in *RAC2* result in reduced actin polymerization, chemotaxis, and neutrophil oxidative burst after *N*-formylmethionyl-leucyl-phenylalanine stimulation.[2,3] In contrast, the patients' neutrophils demonstrated increased filamentous actin content and an increased respiratory burst after *N*-formylmethionyl-leucyl-phenylalanine stimulation compared with controls (Fig 1, *G* and *H*). The patients' cells had a normal oxidative burst at baseline and after phorbol 12-myristate 13-acetate stimulation, both of which are independent of RAC2 (Fig 1, *H*).[1-3]

Transgenic mice expressing the constitutively active $RAC2^{G12V}$ or $RAC2^{Q61L}$ mutants demonstrate thymocyte and T-cell apoptosis.[1] Our patients had lymphopenia with a paucity of naive T cells, reduced recent thymic emigrants, and an accumulation of senescent $CD8^+CD57^+$ T cells (Table I). The patients' unstimulated and TCR-stimulated T cells demonstrated increased apoptosis *in vitro* (Fig. 1, *I*). In addition, EBV-transformed B cells available from patients 2 and 3 demonstrated decreased viability after serum starvation (Fig E1, *C*), mirroring their *in vivo* B-cell lymphopenia. Several mechanisms may contribute to the impaired survival of the patients' T and B cells. Filamentous actin accumulation is known to reduce mitochondrial membrane potential, increase reactive oxidant species, and trigger proapoptotic pathways, all of which increased susceptibility to apoptosis.[8] In addition, the conserved Switch 1 domain in the Rac guanosine triphosphatases binds to the p100β catalytic subunit and activates phosphoinositide-3-kinase (PI3K).[9] PI3K overactivation, due to germline gain-of-function mutations in *PIK3CD* or *PIK3R1*, results in a combined immunodeficiency with certain features shared by our patients, including reduced percentages of naive T cells, the accumulation of senescent $CD8^+CD57^+$ lymphocytes, and increased T- and B-cell apoptosis.[10] The lymphopenia in patients with PI3K overactivation has been attributed to TCR-mediated apoptotic signaling as well as metabolic shifts that favor the expansion of memory and senescent T cells over naive cells.[10] However, because patients with activated phosphoinositide 3-kinase δ syndrome have additional features, including increased IgM levels, lymphoproliferative disease, and autoimmunity, additional patients and studies are needed to investigate the PI3K-AKT axis in patients with gain-of-function mutations in *RAC2*. Patients 2

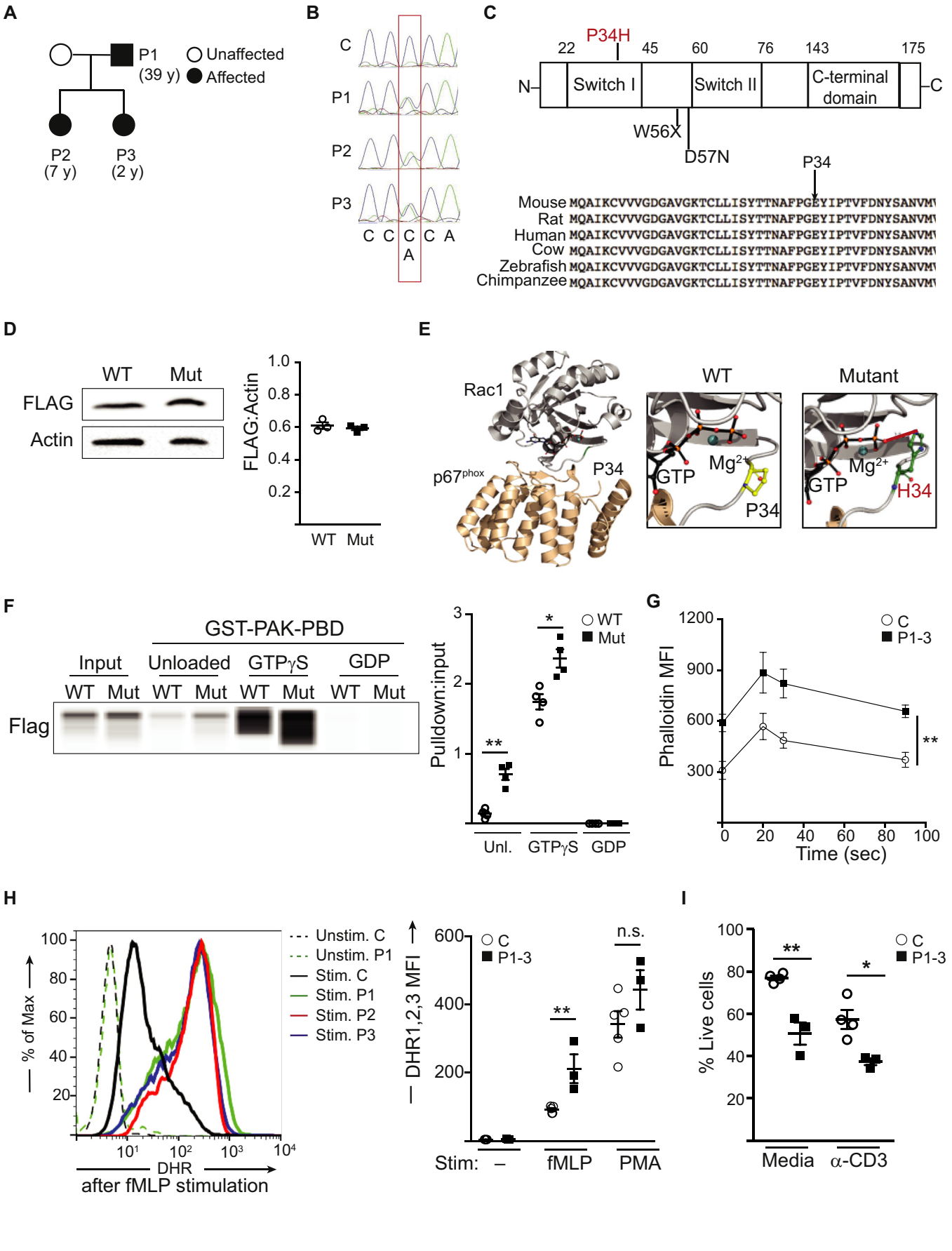
A
P1
(39 y)
Unaffected
Affected
P2
(7 y)
P3
(2 y)
B
C
P1
P2
P3
C C C C A
A
C
P34H
22
45
60
76
143
175
N
Switch I
Switch II
C-terminal domain
C
W56X
D57N
P34
Mouse MQAIKCVVVGDGAVGKTCLLISYTTNAFPGEYIPTVFDNYSANVM
Rat MQAIKCVVVGDGAVGKTCLLISYTTNAFPGEYIPTVFDNYSANVM
Human MQAIKCVVVGDGAVGKTCLLISYTTNAFPGEYIPTVFDNYSANVM
Cow MQAIKCVVVGDGAVGKTCLLISYTTNAFPGEYIPTVFDNYSANVM
Zebrafish MQAIKCVVVGDGAVGKTCLLISYTTNAFPGEYIPTVFDNYSANVM
Chimpanzee MQAIKCVVVGDGAVGKTCLLISYTTNAFPGEYIPTVFDNYSANVM
D
WT
Mut
FLAG
Actin
FLAG:Actin
1.0
0.8
0.6
0.4
0.2
WT Mut
E
Rac1
p67phox
P34
WT
Mutant
GTP
Mg2+
P34
GTP
Mg2+
H34
F
GST-PAK-PBD
Input
Unloaded
GTPγS
GDP
WT Mut WT Mut WT Mut WT Mut
Flag
Pulldown:input
3
2
1
WT
Mut
**
*
Unl.
GTPγS
GDP
G
1200
900
600
300
C
P1-3
Phalloidin MFI
**
0 20 40 60 80 100
Time (sec)
H
100
80
60
40
20
% of Max
10¹ 10² 10³ 10⁴
DHR
after fMLP stimulation
Unstim. C
Unstim. P1
Stim. C
Stim. P1
Stim. P2
Stim. P3
DHR1,2,3 MFI
600
400
200
C
P1-3
**
n.s.
Stim: – fMLP PMA
I
100
80
60
40
20
% Live cells
**
*
C
P1-3
Media
α-CD3

TABLE I. Immune phenotyping of the patients' lymphocytes

Variable	Patient 1	Patient 2	Patient 3
Age at the time of testing (y)	31	7	2
Hemogram (normal range)			
Hemoglobin (g/dL)	**15.6** (10.9-15)	12.6 (10.5-13.8)	11.8 (11-12.8)
WBCs (10^3 cells/μL)	3.670 (5.8-9.3)	**1.640** (5.4-9.7)	**2.960** (5.9-10.4)
Neutrophils (10^3 cells/μL)	**2.822** (3.3-6.3)	**0.730** (2.5-5.9)	**1.557** (2.5-6)
Lymphocytes (10^3 cells/μL)	**0.499** (1.14-2.28)	**0.350** (1.28-2.76)	**0.400** (1.33-4.77)
Monocytes (10^3 cells/μL)	**0.184** (0.29-0.7)	**0.172** (0.19-0.81)	0.266 (0.19-0.94)
Platelets (10^3 cells/μL)	**153** (174-333)	214 (187-367)	216 (208-413)
Lymphocyte subsets			
$CD3^+$ (10^3 cells/μL)	**359** (1000-2600)	**248** (1400-3700)	**252** (2100-6200)
$CD3^+CD4^+$ (10^3 cells/μL)	**72** (530-1500)	**140** (700-2200)	**98** (1300-3400)
$CD45RA^+CD31^+$ recent thymic emigrants, % $CD4^+$	**0.0** (9.8-43)	**32** (45-63)	**29** (57-76)
$CD45RA^+CCR7^+CD31^-$ naive, % $CD4^+$	**0.7** (21-61)	**36.4** (57.1-84.8)	**32.7** (65-84)
$CD45RA^-CCR7^-$ effector memory, % $CD4^+$	**95.8** (7.6-25)	**44.1** (3.3-15.2)	**35.7** (2.9-9.8)
$CD45RA^-CCR7^+$ central memory, % $CD4^+$	**3.3** (26-62)	16.9 (11.2-26.7)	**29.8** (10-22.3)
$CD3^+CD8^+$ (10^3 cells/μL)	**224** (330-1100)	**55** (490-1300)	**65** (620-2000)
$CD45RA^+CCR7^+CD31^-$ naive, % $CD8^+$	**0.4** (11-66)	**4.6** (28-80)	**14.7** (39-89)
$CD45RA^-CCR7^-$ effector memory, % $CD8^+$	**60.9** (16-54)	**56.2** (6.2-29.3)	**36.4** (3.4-28)
$CD45RA^-CCR7^+$ central memory, % $CD8^+$	**0.8** (3.7-32)	1.2 (1.2-4.5)	6.3 (1-5.7)
$CD45RA^+CCR7^-$ TEMRA, % $CD8^+$	38.1 (5.6-43)	38 (9.1-49.1)	**42.7** (4.8-30)
$CD57^+$, % $CD8^+$*	**67.9** (2-38)	**50** (2-20)	**42.8** (2-16)
$CD19^+$ (10^3 cells/μL)	**12** (110-570)	**40** (390-1400)	**19** (720-2600)
$CD27^-IgD^+IgM^+$ naive, % $CD19^+$	60.8 (48-97)	**30.2** (47-77)	**25.0** (54-88)
$CD27^+IgD^+$ unswitched memory, % $CD19^+$	**27.4** (7-23)	8.8 (5.2-20.4)	11.9 (2.7-19)
$CD27^+IgD^-$ switched memory, % $CD19^+$	9.4 (8.8-27)	21.7 (10.9-30.4)	**19.6** (3.3-7.4)
$CD38^{hi}IgM^{hi}$transitional, % $CD19^+$	0.8 (2.2-13)	**35.6** (7.2-23)	**37.8** (10-30)
$CD3^-CD56^+$ (10^3 cells/μL)	101 (70-480)	**56** (130-0.720)	**116** (160-920)
Immunoglobulins			
IgG (mg/dL)	804† (639-1349)	**353** (463-1236)	**239** (345-1213)
IgM (mg/dL)	83 (56-352)	**14** (43-196)	**12** (14-106)
IgA (mg/dL)	226 (70-312)	**17** (25-154)	**13** (43-173)
Tetanus vaccine titer	n.d. before IVIG started	**UD**	**UD**
Hepatitis vaccine titer	n.d. before IVIG started	**UD**	**UD**
Proliferation‡			
Anti-CD3 (% $CD4^+$ divided)	**65.3** (84.2-93.8)	89.05 (84.2-93.8)	**24.5** (84.2-93.8)
Phytohemmaglutinin (% $CD4^+$ divided)	**6.04** (62.9-85)	**60** (62.9-85)	63.85 (62.9-85)
Anti-CD3 (% $CD8^+$ divided)	**54.5** (87-92.7)	**64.45** (87-92.7)	**34.3** (87-92.7)
Phytohemmaglutinin (% $CD8^+$ divided)	**3.81** (83.1-93.5)	**21.6** (83.1-93.5)	**20.75** (83.1-93.5)

IVIG, Intravenous immunoglobulin; *n.d.*, not done; *UD*, undetectable; *WBC*, white blood cell.
Boldface values are outside the normal range.
*Daball et al.[6]
†On IVIG.
‡Reference range is for 3 healthy controls done on the day of the study.

FIG 1. RAC^{P34H} is a gain-of-function mutant. **A,** Pedigree. **B,** Sanger sequencing of the P34H mutation in *RAC2*. **C,** Linear schematic of RAC2 with P34H mutation (red) and loss-of-function mutations (W56X and D57V), with the corresponding amino acid sequence for indicated species. **D,** Representative immunoblot and densitometry quantification from 3 independent experiments of HEK293T cells transfected with constructs encoding Flag-RAC2 (WT) or Flag-$Rac2^{P34H}$ (Mut). **E,** Ribbon diagram of WT or $RAC1^{P34H}$ with the effector protein $p67^{phox}$. Only the crystal structure of the activated RAC1 Switch I region, which is identical to that of RAC2, has been solved. The red line indicates a potential new hydrogen bond. **F,** Representative capillary immunoblot of lysates from FLAG-Rac2 pull-down assays. GST-PAK-PDB is a fusion protein of GST and the Rac/Cdc42 binding domain (PBD) of human p21 activated kinase 1 protein (PAK). Densitometry is pooled from 4 independent experiments. **G,** Mean fluorescence intensity (MFI) of phalloidin in neutrophils from P1 to P3 or 5 controls (C) after fMLP stimulation, $^{**}P < .01$ by 2-way ANOVA. **H,** Oxidative burst in dihydrorhodamine 123-loaded neutrophils from P1 to P3 and 5 controls after stimulation with fMLP or PMA. **I,** Percentage of live $CD3^+$ T cells from P1 to P3 and 4 controls with indicated stimulus. Data from *G*, *H*, and *I* are representative of 1 of 2 independent experiments. For all data shown, $^*P < .05$, $^{**}P < .01$ by 1-way ANOVA with Holm-Šídák unless otherwise indicated. *fMLP*, *N*-Formylmethionyl-leucyl-phenylalanine; *Mut*, mutant; *n.s.*, nonsignificant; *P1*, patient 1; *P2*, patient 2; *P2*, patient 3; *PMA*, phorbol 12-myristate 13-acetate; *Stim.*, stimulated; *Unstim.*, unstimulated.

and 3 also had features not seen in patient 1, such as reduced naive B cells and increased transitional B cells. Some of the variability in the immune phenotypes among the 3 patients may result from the exposure of patient 1 to chemotherapy, the age differences among the patients, or intrafamilial genetic variations.

The data presented here provide a counterpoint to previous studies of patients with the dominant negative $RAC2^{D57N}$ mutant. Although impaired neutrophil function and chemotaxis are the hallmarks of loss-of-function variants in *RAC2*, we show that patients with a monoallelic activating *RAC2* mutation have increased actin polymerization, exaggerated neutrophilic oxidative burst, lymphopenia, and increased lymphocyte apoptosis. This combined immunodeficiency indicates the importance of regulating RAC2 activity for intact immune function.

We are grateful to the patients, the patients' families, and the nurses for their participation in this study. We thank David Williams and members of his laboratory for helpful discussions.

Vassilios Lougaris, MD[a]*
Janet Chou, MD[b]*
Abdallah Beano, MD[b]
Jacqueline G. Wallace, BSPH[b]
Manuela Baronio, PhD[a]
Luisa Gazzurelli, PhD[a]
Tiziana Lorenzini, MD[a]
Daniele Moratto, PhD[c]
Giovanna Tabellini, PhD[d]
Silvia Parolini, PhD[d]
Michael Seleman[b]
Kelsey Stafstrom, MS[b]
Haiming Xu, PhD[e]
Chad Harris, MS[e]
Raif S. Geha, MD[b]‡
Alessandro Plebani, MD, PhD[a]‡

From [a]the Pediatrics Clinic and Institute of Molecular Medicine "A. Nocivelli," Department of Clinical and Experimental Sciences, University of Brescia and ASST Spedali Civili of Brescia, Brescia, Italy; [b]the Division of Immunology, Boston Children's Hospital and Harvard Medical School, Boston, Mass; [c]the Institute for Molecular Medicine A. Nocivelli, Department of Pathology, Laboratory of Genetic Disorders of Childhood, Department of Molecular and Translational Medicine, University of Brescia, ASST Spedali Civili of Brescia, Brescia, Italy; [d]the Department of Molecular and Translational Medicine, University of Brescia, Brescia, Italy; and [e]Boston Children's Hospital and Dana-Farber Cancer Institute, Harvard Medical School and Harvard Stem Cell Institute, Boston, Mass. E-mail: vlougarisbs@yahoo.com. Or: Raif.Geha@childrens.harvard.edu.

*These authors contributed equally to this work.
‡These authors contributed equally to this work.

This study was funded by the European Community's Seventh Framework Programme (grant no. FP7/2007-2013 201549 to V.L. and A.P.), EURO-PADnet HEALTH (grant no. F2-2008-201549 to V.L. and A.P.), Italian Ministerial Grant (grant no. GR-2010-2315762 to V.L. and A.P.), Fondazione C. Golgi, Brescia, Italy (V.L. and A.P.), the Jeffrey Modell Foundation (V.L. and A.P.); the Perkin Fund (R.S.G. and J.C.); and the National Institutes of Health (grant nos. AI124101 and AI139633 to R.S.G. and grant no. 5K08AI116979 to J.C.).

Disclosure of potential conflict of interest: The authors declare that they have no relevant conflicts of interest.

REFERENCES

1. Pai S-Y, Kim C, Williams DA. Rac GTPases in human diseases. Dis Markers 2010; 29:177-87.
2. Ambruso DR, Knall C, Abell AN, Panepinto J, Kurkchubasche A, Thurman G, et al. Human neutrophil immunodeficiency syndrome is associated with an inhibitory Rac2 mutation. Proc Natl Acad Sci U S A 2000;97:4654-9.
3. Williams DA, Tao W, Yang F, Kim C, Gu Y, Mansfield P, et al. Dominant negative mutation of the hematopoietic-specific Rho GTPase, Rac2, is associated with a human phagocyte immunodeficiency. Blood 2000;96:1646-54.
4. Alkhairy OK, Rezaei N, Graham RR, Abolhassani H, Borte S, Hultenby K, et al. RAC2 loss-of-function mutation in 2 siblings with characteristics of common variable immunodeficiency. J Allergy Clin Immunol 2015;135:1380-4.e5.
5. Accetta D, Syverson G, Bonacci B, Reddy S, Bengtson C, Surfus J, et al. Human phagocyte defect caused by a Rac2 mutation detected by means of neonatal screening for T-cell lymphopenia. J Allergy Clin Immunol 2011;127:535-8, e1-2.
6. Cura Daball P, Ventura Ferreira MS, Ammann S, Klemann C, Lorenz MR, Warthorst U, et al. CD57 identifies T cells with functional senescence before terminal differentiation and relative telomere shortening in patients with activated PI3 kinase delta syndrome. Immunol Cell Biol 2018;96:1060-71.
7. Kircher M, Witten DM, Jain P, O'Roak BJ, Cooper GM, Shendure J. A general framework for estimating the relative pathogenicity of human genetic variants. Nat Genet 2014;46:310-5.
8. Desouza M, Gunning PW, Stehn JR. The actin cytoskeleton as a sensor and mediator of apoptosis. Bioarchitecture 2012;2:75-87.
9. Fritsch R, de Krijger I, Fritsch K, George R, Reason B, Kumar MS, et al. RAS and RHO families of GTPases directly regulate distinct phosphoinositide 3-kinase isoforms. Cell 2013;153:1050-63.
10. Cannons JL, Preite S, Kapnick SM, Uzel G, Schwartzberg PL. Genetic defects in phosphoinositide 3-kinase δ influence CD8+ T cell survival, differentiation, and function. Front Immunol 2018. https://doi.org/10.3389/fimmu.2018.01758. eCollection 2018 [Epub ahead of print].

https://doi.org/10.1016/j.jaci.2019.01.001

METHODS

Flow cytometric analysis of T cells, B cells, natural killer cells, and neutrophils

Antibodies used for flow cytometry studies of T and B cells were as follows: anti-CD45RA FITC, anti-IgD FITC, anti-CD56 PE, anti-CD31 PE, anti-CD38 PerCP-Cy5.5, anti-CD3 PE-Cy7, anti-CD27 PE-Cy7, anti-CD4 APC, anti-CD8 APC-H7, anti-IgM Bv421, anti-CCR7 Bv421, anti-CD45 V500 Bv510, and anti-CD19 Bv510, all manufactured by Becton Dickinson (Franklin Lakes, NJ). Immunophenotyping of natural killer (NK) cells was done using the following antibodies: BAB281 (IgG_1, anti-NKp46); AZ20 (IgG_1, anti-NKp30); and anti-CD3 FITC and anti-CD56 PC5, anti-CD14 FITC, and anti-CD20 FITC (Beckman Coulter, Immunotech, Marseille, France). NK-cell analysis was performed by gating on $CD56^+CD3^-CD14^-CD20^-$ cells. For assessment of CD11b and CD62L expression on neutrophils, whole blood samples from patients and controls were stained either with or without activation with phorbol 12-myristate 13-acetate (300 ng/mL) for 30 minutes at 37°C using anti-CD45 APC, anti-CD11b FITC, and anti-CD62L PerCP (all BD Pharmingen, San Diego, Calif). Analyses were performed using the FlowJo software version 8.8.7 (TreeStar, Ashland, Ore).

T-cell proliferation studies

T-cell proliferation was quantified using dilution of carboxyfluorsecein diacetate succinimidyl ester (Thermo Fisher Scientific, Waltham, Mass) after stimulation with anti-CD3 (10 μg/μL) (Sigma-Aldrich, St Louis, Mo) or PHA (5 ng/μL) (Sigma-Aldrich) as previously described.[E1]

Whole-exome sequencing

Whole-exome sequencing was performed on genomic DNA from all 3 patients using the Illumina HiSeq-2000 (Illumina Inc, San Diego, Calif), using Agilent SureSelect for library preparation. The average coverage of the exome was 173×. The Burrows-Wheeler Aligner was used to map reads to the human reference genome assembly GRCh37.[E2] Variants were called using the Genome Analysis Toolkit.[E3]

Sanger sequencing

Sanger sequencing of the P34H mutation in Exon 2 of *RAC2* was performed with the following primers: (F: 5′-CTTGCAGGCTCTCGGGTGTG-3′, R: 5′-GTGCTGCCTTCTTGGCTGGA -3') with ABI PRISM 310 (Thermo Fisher Scientific).

Immunoblotting

Lysates from T-cell blasts, BLCL, or transfected HEK293T cells were lysed in RIPA buffer (Millipore, Burlington, Mass), 50 mM EDTA (Thermo Fisher Scientific), and protease inhibitors (Thermo Fisher Scientific). Electrophoresis of lysates was performed on 4% to 12% precast polyacrylamide gels (Thermo Fisher Scientific), followed by immunoblotting with the following antibodies as indicated in figure legends: anti-Rac2 (AT2G1, Abcam, Cambridge, United Kingdom), anti-FLAG (F3165, Sigma-Aldrich), anti–β-actin (Sigma-Aldrich).

Rac2 pull-down activation assay

HEK293T cells were transfected with either N-terminal FLAG-tagged WT Rac2 (Genecopoeia) or the $Rac2^{P34H}$ mutant, which was generated using the QuikChange II XL Site-Directed Mutagenesis kit (Agilent, Santa Clara, Calif). Two days after transfection using the TransIT-LT1 transfection reagent (Mirus Bio, Madison, Wis), cells were lysed in 25 mM HEPES, 150 mM NaCl, 1% IGEPAL CA-630, 10 mM $MgCl_2$, 1 mM EDTA, 2% glycerol, and EDTA-free Protease Inhibitor Cocktail (Roche, Basel, Switzerland). To prepare guanosine triphosphate γS– or guanosine diphosphate–loaded controls, 10 mM EDTA was added to lysates, followed by 0.1 mM of guanosine triphosphate γS (Abcam) or 1 mM of guanosine diphosphate (Sigma-Aldrich) for 15 minutes at 37°C. Loading was stopped by the addition of 65 mM $MgCl_2$. Active RAC2 was pulled down from a portion of the lysates by incubating with PAK-PBD beads (Cytoskeleton), followed by washing and immunoblotting using capillary Western blotting (ProteinSimple) and anti-FLAG antibody (Sigma-Aldrich).

Studies of oxidative burst in neutrophils

Whole blood from patients and controls was stimulated with *N*-formylmethionyl-leucyl-phenylalanine (1 μM) or phorbol 12-myristate 13-acetate (300 ng/mL), followed by Dihydrorhodamine 123 staining as previously described.[E4]

Studies of actin polymerization in neutrophils

Whole blood purified neutrophils from patients and controls were left untreated or stimulated with *N*-formylmethionyl-leucyl-phenylalanine (1 μM) for indicated times, followed by fixation and staining with fluorescein isothiocyanate–conjugated phalloidin (Sigma-Aldrich) per the manufacturer's guidelines.

Apoptosis assays

Apoptosis was determined in peripheral T cells from controls or patients, with or without anti-CD3 stimulation (10 μg/μL) (Sigma-Aldrich) for 48 hours. Apoptosis was assessed in EBV-immortalized B cells from controls or patients without stimulation. Live cells were identified by the absence of staining for either Annexin V or propidium iodide. (eBioscience, San Diego, Calif).

Statistics

For all graphs, each point in the scatterplots depicted represents a biologic replicate: each control point corresponds to a different healthy individual and each patient point corresponds to a different patient. Student *t* test was used for comparisons of 2 groups; 1- or 2-way ANOVA with the Holm-Šídák postcomparison test was used for the comparison of more than 2 groups, as indicated. Data are graphed as mean with SEM. Statistical analysis was performed using GraphPad Prism.

REFERENCES

E1. Lanzi G, Moratto D, Vairo D, Masneri S, Delmonte O, Paganini T, et al. A novel primary human immunodeficiency due to deficiency in the WASP-interacting protein WIP. J Exp Med 2012;209:29-34.
E2. Li H, Durbin R. Fast and accurate short read alignment with Burrows–Wheeler transform. Bioinformatics 2009;25:1754-60.
E3. DePristo MA, Banks E, Poplin R, Garimella KV, Maguire JR, Hartl C, et al. A framework for variation discovery and genotyping using next-generation DNA sequencing data. Nat Genet 2011;43:491-8.
E4. Chen Y, Junger WG. Measurement of oxidative burst in neutrophils. Methods Mol Biol Clifton NJ 2012;844:115-24.

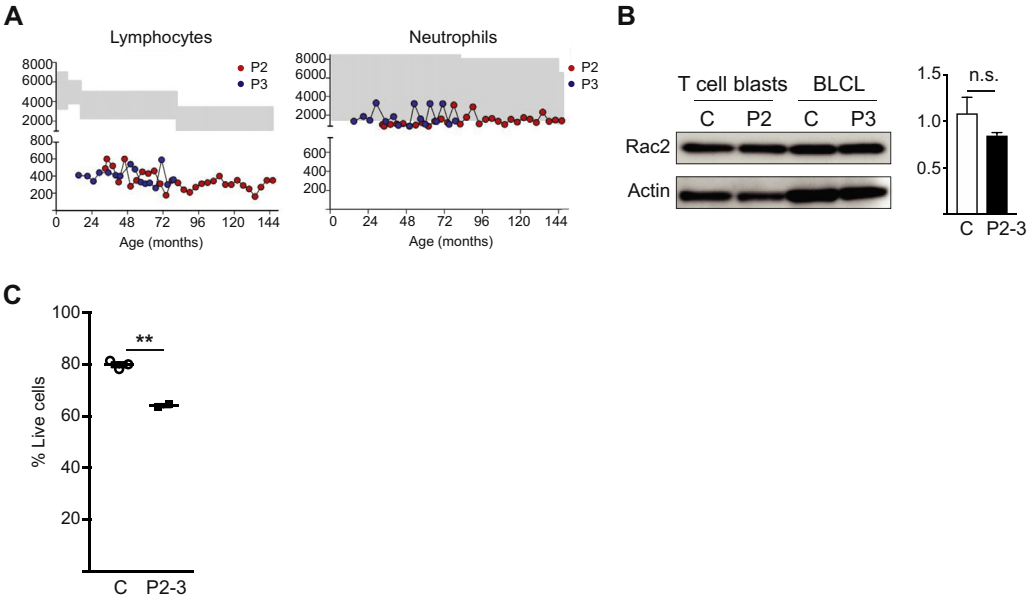

FIG E1. A, Absolute lymphocyte and neutrophil counts of P2 and P3. **B,** Representative immunoblot of RAC2 and actin in T-cell blasts and EBV-transformed B-cell lymphoblastic cells lines from P2 and P3 and 2 controls. Quantification was obtained from 2 independent experiments. **C,** Percentage of live EBV-transformed B cells from P2 and P3 and 3 controls, pooled from 2 independent experiments. *n.s.*, Not significant; *P2*, patient 2; *P3*, patient 3. $^{**}P < .01$ by Student *t* test.

TABLE E1. Variants shared by all 3 patients, which are rare (<30 alleles in gnomAD) and deleterious (CADD PHRED-like score >15)

Chromosome	Position	Reference	Patient	Consequence	Gene name	CADD score
1	3328670	A	C	Non-synonymous	*PRDM16*	19.7
1	22310701	C	A	Non-synonymous	*CELA3B*	19.63
1	27023871	G	T	Non-synonymous	*ARID1A*	21.1
1	27679943	C	T	Non-synonymous	*SYTL1*	34
1	27695833	C	T	Non-synonymous	*FCN3*	23.3
1	27695833	C	T	Upstream	*MAP3K6*	23.3
2	220420994	G	A	Non-synonymous	*OBSL1*	32
3	100373932	G	A	Non-synonymous	*GPR128*	18.75
5	40681232	G	T	Non-synonymous	*PTGER4*	33
5	79354543	G	A	Non-synonymous	*THBS4*	23.9
5	102887994	A	G	Non-synonymous	*NUDT12*	24.2
5	112884695	G	A	Non-synonymous	*YTHDC2*	22.9
5	137713429	C	A	Non-synonymous	*KDM3B*	17.27
5	147796767	G	A	Non-synonymous	*FBXO38*	27.8
5	150227995	T	A	Non-synonymous	*IRGM*	22.7
9	1052014	G	T	Non-synonymous	*DMRT2*	33
9	121976315	T	A	Non-synonymous	*BRINP1*	16.83
9	130826079	C	G	Upstream	*SLC25A25*	22.1
9	130826079	C	G	Non-synonymous	*NAIF1*	22.1
9	140057403	G	C	Non-synonymous	*GRIN1*	24
10	14870199	A	G	Non-synonymous	*CDNF*	24.3
10	71966072	G	A	Non-synonymous	*PPA1*	22.9
12	10962022	C	T	Non-synonymous	*TAS2R9*	15.52
12	10962022	C	T	Upstream	*TAS2R8*	15.52
12	29786258	T	C	Non-synonymous	*TMTC1*	29.3
12	56030724	T	G	Non-synonymous	*OR10P1*	22.1
12	57578143	C	T	Non-synonymous	*LRP1*	22.4
14	21780617	A	G	Non-synonymous	*RPGRIP1*	27.3
14	47600951	A	T	Non-synonymous	*MDGA2*	22.5
14	72196852	C	G	Non-synonymous	*SIPA1L1*	22.6
17	26684394	T	G	Upstream	*TMEM199*	15.59
19	1592525	A	C	Non-synonymous	*MBD3*	28.3
19	1592543	G	C	Non-synonymous	*MBD3*	23.3
19	6452423	C	T	Non-synonymous	*SLC25A23*	19.64
19	44662108	A	G	Non-synonymous	*ZNF234*	25
19	50832152	T	C	Upstream	*NR1H2*	16.25
19	50832152	T	C	Non-synonymous	*KCNC3*	16.25
22	24953707	C	T	Upstream	*GUCD1*	22.8
22	24953707	C	T	Non-synonymous	*SNRPD3*	22.8
22	**37637633**	**G**	**T**	**Non-synonymous**	***RAC2***	**32**

CADD, Combined Annotation Dependent Depletion.
The *RAC2* variant is listed in boldface.